CFD Simulation of Liquid-Liquid Extraction Columns and Visualization of Eulerian Datasets

Mark W. Hlawitschka[1,4], Fang Chen[2,4], Hans-Jörg Bart[1,4], and Bernd Hamann[3]

1 **Chair of Separation Science and Technology, University of Kaiserslautern, Germany**
mark.hlawitschka@mv.uni-kl.de, bart@mv.uni-kl.de
2 **Computer Graphics and HCI Group, University of Kaiserslautern, Germany**
chen@informatik.uni-kl.de
3 **Institute for Data Analysis and Visualization & CS Department University of California, Davis, USA** hamann@ucdavis.edu
4 **Center for Mathematical and Computational Modelling (CM)^2, University of Kaiserslautern, Germany**

Abstract

In this joint work, a complete framework for modeling, simulating and visualizing multiphase fluid flow within an extraction column is presented. We first present a volume-of-fluid simulation, which is able to predict the surface of the droplets during coalescence. However, a fast and efficient model is needed for the simulation of a liquid-liquid extraction column due to the high number of occurring droplets. To simulate the velocity and droplet size in a DN32 extraction column, a coupled computational fluid dynamic-population balance model solver is used. The simulation is analyzed using path-line based visualization techniques. A novel semi-automatic re-seeding technique for droplet path-line integration is proposed. With our technique, path-lines of fluid droplets can be re-initialized after contact with the stirring devices. The droplet breakage is captured, allowing the engineer to improve the design of liquid-liquid columns layout.

1998 ACM Subject Classification I.6.6 Simulation Output Analysis

Keywords and phrases computational fluid dynamics, multiphase fluid, droplet collision, Eulerian, path-line

Digital Object Identifier 10.4230/OASIcs.VLUDS.2011.59

1 Introduction

In chemical industry, liquid-liquid extraction is an important separation technique based on the relative solubilities of the compounds in two different immiscible liquids. It is mainly applied when distillation is impractical (similar boiling points of the materials) or the mixtures contain temperature sensitive compounds. The efficiency of the column is mainly influenced by the choice of the solvent and by the hydrodynamics inside the column. The characterization of the hydrodynamics without experiments was made possible through the use of computational fluid dynamics (CFD). Multiphase flow is commonly simulated by the use of the volume-of-fluid (VOF) model, Euler-Euler model or Euler-Lagrange model. VOF allows a tracking of the dispersed phase surface but requires a detailed resolution of the droplet and its curvature by the computational mesh. Due to this, it is mainly used for the investigation of single droplet interactions. The Euler-Lagrange method is limited by the

Proceedings of IRTG 1131 – Visualization of Large and Unstructured Data Sets Workshop 2011.
Editors: Christoph Garth, Ariane Middel, Hans Hagen; pp. 59–70

OpenAccess Series in Informatics
Schloss Dagstuhl – Leibniz-Zentrum für Informatik, Dagstuhl Publishing, Germany


phase fraction and requires a higher computational load compared to the Euler-Euler model. Therefore, the Euler-Euler model still is the workhorse for dispersed multiphase simulations.

The simulation of extraction columns with CFD started with Rieger et al. [3], who used the CFD Code Fire for single-phase simulations of an extraction column of type rotating disc contactor (RDC). Modes & Bart [4] used the code FIDAP to perform two-phase simulations. The droplet size change in an RDC column was accounted by Vikhansky & Kraft [5] and Drumm & Bart [6] using population balance models. Whereas Drumm & Bart [6] mainly focuses on the moment based population balances, Vikhansky & Kraft [5] used the Monte Carlo method. Hlawitschka et al. [7] transferred the results of Drumm [8] to a three-dimensional test case of a Kühni extraction column. For population balance modeling, a one-group model (OPOSPM) is used which guarantees a low computational time and a good prediction of the hydrodynamics and flow field [9]. An adaption of the coalescence and breakage kernels using models from Martínez-Bazán et al. [10], Prince & Blanch [11] and Luo & Svendsen [12] was investigated by Hlawitschka & Bart [13].

In this paper, the volume-of-fluid method is used to illustrate a binary droplet coalescence and to show up the challenges for a whole column simulation. In a next step, a coupled CFD-population balance code is used to simulate a section of a Kühni Miniplant column using the Eulerian model coupled with a population balance model. In the output of our presented simulation, the interface is not directly tracked and the dispersed phase is only represented by the phase fraction and droplet size within each computational cell. Therefore, a direct analysis of the simulation output (e.g. droplet position) is not possible with the current visualization techniques. The Eulerian model requires an adequate representation scheme of the dispersed phase, which couples both the cell volume fraction as well as the particle size. Recent research on stochastic modeling [14] gives us a pointer on how those two fields can be negotiated and brought together. Apart from droplet distribution in each time step, the dynamic behavior of sets of droplets is of great interest among engineers and researchers. Recent research in fluid visualization has shown that line integrals have been helpful visual tools in tracking fluid particles [15, 16, 17]. Aside from accurate computation of line integrals, the start and end points of a droplet path should be handled with special care in the extraction column, since fluid droplet break or merge along their path. A novel re-seeding approach for capturing droplet path-lines for time-varying multiphase flow field is proposed.

2 Binary Droplet Coalescence

2.1 Numerical Background

To illustrate the basic droplet coalescence, we simulate a binary droplet coalescence using the open source CFD tool OpenFOAM. In our implementation, we used a volume-of-fluid type of solver, called multiphaseInterFoam. This method is combined with dynamic mesh refinement for a better resolution of the droplet interface. Due to the VOF model theory, a direct contact of the droplets leads to a direct coalescence of the droplets. The VOF model was applied by several groups to simulate bubble coalescence [18, 19, 20] and also applied for droplet coalescence [21]. A droplet in the VOF method is represented by the volume fraction α, which is given by:

- surrounding phase for $\alpha = 0$
- droplet for $\alpha = 1$
- existence of an interphase when $0<\alpha<1$

The transport of mass is described by the continuity equation

$$\frac{\partial}{\partial t}\alpha + \nabla(\alpha \mathbf{u}) = 0, \tag{1}$$

where the velocity is given by $\mathbf{u}$. In addition, a single momentum equation is used for the mixture of two-phase-fluid. The viscosity and the density of the mixture is expressed by

$$\begin{aligned} \mu &= \alpha_2\mu_2 + (1-\alpha_2)\,\mu_1 \\ \rho &= \alpha_2\rho_2 + (1-\alpha_2)\,\rho_1 \end{aligned} \tag{2}$$

The momentum equation hence is described by

$$\frac{\partial}{\partial t}(\rho\mathbf{u}) + \nabla\cdot(\rho\mathbf{u}\mathbf{u}) + \nabla\mathbf{u}\cdot\nabla[\mu] = -\nabla p + \mathbf{F}, \tag{3}$$

where $\mathbf{F}$ is the surface tension force $\mathbf{F} = \sigma\kappa(x)\mathbf{n}$. κ is the curvature of the interface and $\mathbf{n}$ is a unit vector normal to the interface.

2.2 Numerical Setup

The grid is generated using the open source grid generator blockMesh creating a total simulation area of size x=0.01 m, y= 0.006 m and z=0.006 m. The initial mesh is generated with 200 cells in x-axis, 120 cells in y-axis and 120 cells in z-axis. The boundaries of the mesh are defined by a zero gradient boundary condition. The two toluene droplets (ρ=866 kg/m^3, ν=6.3$\cdot$ 10^{-7}m^2/s) are defined by spherical set functions defining a phase fraction of 1 in a radius of 0.002 m around the locations (-0.004,0,0) and (0.004,0,0) that represent the center of the droplets. The surrounding liquid is defined as water. The surface tension between the droplets and the water is set to 35 mN. A dynamic mesh refinement is used to refine the interface of the droplets in advance of the simulation and during the simulation. The upper refine level based on the volume fraction is set to 0.999, while the lower is set to 0.1. Forty buffer layers were used to generate a smooth mesh. In each refinement step, the maximum refinement is set to 20 resulting in an initial mesh of 3 million cells. The time step is set to 10^{-5} s and the simulation is run to simulate 0.25 s until the droplets coalesce and a new round droplet is formed. Each of the two droplets has an initial velocity of 0.1 m/s in the direction towards the other droplet. Gravity is neglected in order to ensure droplet motion only in the x-axis direction.

2.3 Binary Droplet Coalescence Result

The simulated droplet coalescence is shown in Fig. 1. The droplets come in touch with each other after 42 ms and a liquid bridge is formed. The formed droplet changes its shape from a bar-bell at 50 ms (b), to a citrus form at 62 ms (c), over a sphere form at 70 ms (d) to a dented form at 75 ms (e). The droplet is elongated again in x-axis to a cylindrical form at (100 ms) (f) and changes to an oval droplet at 0.12 s (g) and back to the round sphere form at 160 ms (g). The droplet is stretched again at 180 ms (h) forms a round droplet at 200 ms (i). The periodic elongation in x-axis decreases with time until the newly generated droplet is stable.

The droplet coalescence can be described in good agreement with literature data [22]. However the first contact of the droplet is still a challenging task. Repulsion effects and delayed coalescence, which describes a coalescence that does not directly start after the initial contact, is still simulated using simplified models based on a contact time and contact

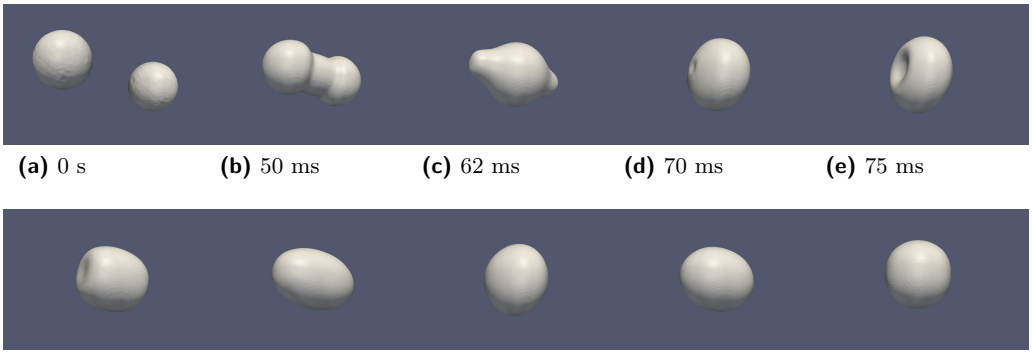

(a) 0 s **(b)** 50 ms **(c)** 62 ms **(d)** 70 ms **(e)** 75 ms

(f) 100 ms **(g)** 120 ms **(h)** 160 ms **(i)** 180 ms **(j)** 200 ms

Figure 1 Droplet coalescence of two 4 mm droplets simulated using the VOF method.

area [21]. In a pilot plant column with diameters of 150 mm, several 100,000s of droplets exist. To model a full column, the number of mesh cells will increase dramatically and exceed the computational resources. Moreover, droplet breakage is becoming problematic to model, because they heavily rely on the mesh size and quality. Hence, a simulation without describing the droplet interface directly is preferred.

While VOF focuses on single droplet boundaries, Eulerian models provide the possibility to simulate complex scenarios with large number of dispersed droplets. In the next section, we present a Eulerian model combined with population balance modeling to simulate the hydrodynamics in a section of a Kühni Miniplant column.

3 Eulerian Modeling

The Eulerian model is part of the Euler-Euler approach, where the phases are treated as interpenetrating continua. The occurring phases are represented by the volume fraction α, which is identical to a statistical probability of the droplets being at a specific position. The sum of the phase fractions of the continuous (c) and dispersed phase (d) has to be 1:

$$\alpha_c + \alpha_d = 1. \tag{4}$$

The transport of the phases is described by the conservation equations and is solved for each phase. The continuity equation consists of the storage term and the convective term on the left hand side of the equation and of a source term on the right hand side of the equation.

$$\frac{\partial(\alpha_c \rho_c)}{\partial t} + \nabla \cdot (\alpha_c \rho_c \mathbf{u}_c) = \rho_c S_c. \tag{5}$$

The momentum balance of the continuous phase is given by:

$$\frac{\partial(\alpha_c \rho_c \mathbf{u}_c)}{\partial t} + \nabla \cdot (\alpha_c \rho_c \mathbf{u}_c \mathbf{u}_c) = -\alpha_c \nabla p + \nabla \tau_l + \alpha_c \rho_c \mathbf{g} + \mathbf{F}_c + \rho_c \mathbf{u}_c S_c. \tag{6}$$

The first term on the left hand side is the rate of change of momentum and the second term is the conservation of momentum. On the right hand side the effect of pressure and stress-strain is given by the first two terms. The interaction of phases is taken into account by the resistance forces $\mathbf{F}_c$. The source term S is set to 0. The momentum balance and continuity equation is formed for the dispersed phase respectively. Analogous to the work of

[23] only the drag force is taken into account as interphase resistance. The mass force and the buoyancy force for liquid-liquid systems can be neglected. The resistance between the continuous phase and the dispersed phase is calculated with the help of the model of Schiller & Naumann [24] for the drag coefficient C_D

$$\mathbf{F}_{c,d} = \frac{3\rho_c\alpha_c\alpha_d C_d|\mathbf{u}_d - \mathbf{u}_c|(\mathbf{u}_d - \mathbf{u}_c)}{4d_d} \tag{7}$$

where

$$C_D = \begin{cases} 24(l + 0.15Re^{0.678})/Re, & Re \leq 1000 \\ 0.44 & Re > 1000. \end{cases} \tag{8}$$

3.1 Droplet Size Calculation

Since the dispersed phase surface is not directly tracked, events such as droplet coalescence and droplet breakage as well as droplet growth cannot be accounted for directly. In the last decade, population balance models in combination with breakup and coalescence kernels became popular to account for these effects. The variable droplet size can be accounted for different models, as represented by the class method or the Quadrature Method of Moments (QMOM). In this work, however, a one group model, the One Primary One Secondary Particle Method, is used [9]. The model calculates the mean droplet size in each cell based on the volumetric diameter and is calculated by the third moment and the zeroth moment:

$$d_{30} = \sqrt[3]{\frac{m_3}{m_0}} = \sqrt[3]{\frac{6\alpha}{\pi m_0}}. \tag{9}$$

The third moment refers to the total volume of the droplets, where the zeroth moment gives the total number of droplets. The number of droplets increases due to breakage and decreases due to coalescence. In addition to the Eulerian modeling, only one additional transport equation has to be added to the solver for the number concentration of the dispersed phase d:

$$\frac{\partial(\alpha_d m_0 \rho_d)}{\partial t} + \nabla \cdot (\alpha_d \rho_d m_0 \mathbf{u_d}) = \alpha_\mathbf{d}\rho_\mathbf{d}\mathbf{S_d}. \tag{10}$$

The source term on the right hand side describes the generation and reduction of the number of droplets. For this description, the coalescence model of Coulaloglou & Tavlarides [2] and the breakage model of Andersson & Andersson [1] are used in this work. The coalescence of two droplets is described by the coalescence efficiency τ and by the coalescence rate h:

$$\begin{aligned} \tau(d_1, d_2) &= \exp(-C_1 \frac{\mu_c \rho_c \epsilon}{\sigma^2}(\frac{d_1 d_2}{d_1 + d_2})^4) \\ h(d_1, d_2) &= C_2 \frac{\epsilon^{1/3}}{1+\alpha}(d_1 + d_2)^2(d_1^{2/3} + d_2^{2/3})^{1/2} \end{aligned} \tag{11}$$

The constants C_1 and C_2 are adjusted to the system of butyl acetate/water. The breakage kernel consists of the breakup rate g, which is given by:

$$g(d) = \int_{d_{0/10}}^{10d_0} \omega_s(d_0, \lambda) P(d_0, \lambda)\, d\lambda \tag{12}$$

The interaction frequency ω_s between a droplet of size d_0 and an eddy of size λ is:

$$\omega_s(d_0, \lambda) = \frac{C_3 \pi d_0^3 \epsilon^{1/3}}{6\lambda^{14/3}}. \tag{13}$$

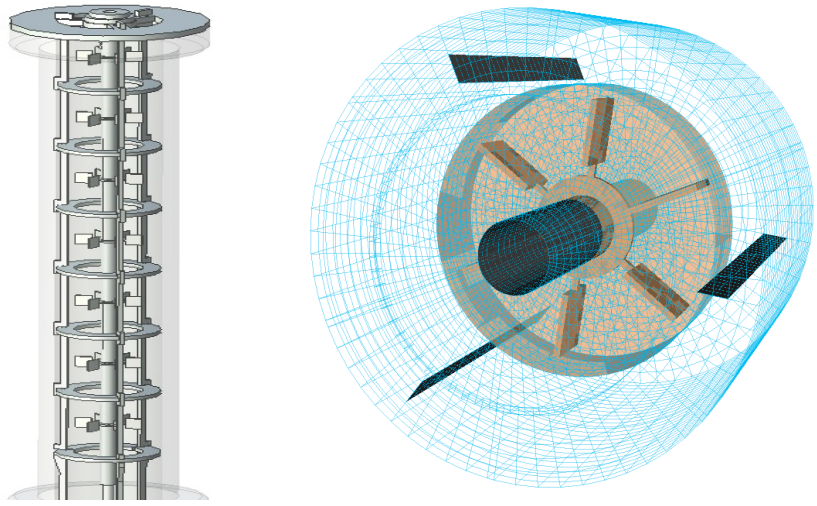

(a) (b)

Figure 2 Column geometry (left) and a visualization of the generated mesh of a single compartment containing the moving reference frame around the stirrer (right).

The constant C_3 is taken from the model of Luo & Svendsen [12] and is 0.822. The probability of an eddy breaking up a fluid particle of size d is given by the integral of the normalized energy distribution $\phi(\chi)$:

$$P(d_0, \lambda) = \int_{\chi_{\min}}^{\infty} \phi(\chi)\, d\chi. \tag{14}$$

χ is defined by the ratio of the eddy viscosity to the average eddy viscosity. In addition to the breakup rate, the available energy by turbulence must be larger than the increase in interfacial energy due to deformation that breakup occurs. In comparison to the direct simulation of a droplet coalescence and breakage, the breakup kernel and coalescence kernel has to account for the fluctuations (e.g. elongation) of the droplets taking place in the real column. Furthermore, surfactants can have an influence to the coalescence and breakage and have to be accounted by the adjustable parameters of the models.

3.2 Mesh and Boundary Conditions

In this section, we describe the geometry of our extraction column, the numerical mesh for simulation and the boundary conditions for solving PBM. For the simulation of a seven-compartment section of a Kühni Miniplant column, a corresponding mesh is built in Gambit resulting in over 500 000 cells. The simulated column geometry is shown in Fig. 2a. An in- an outflow section are added to the numerical mesh at the bottom and top of the column. A closer look inside a single compartment is given in Fig. 2b, where the part around the stirrers is treated as moving reference frame (MRF). In the middle of each compartment, a six-baffled stirrer is installed. Neighboring compartments are separated by two stators, which in this case consist of two metal rings. Three stream-breakers are orientated in an angle of 120° to each other. The volume stream of each phase (water and butyl acetate) is set to 8 l/h and the stirring speed is set to 300 rpm. The constants in the model of Coulaloglou & Tavlarides

[2] are set adequate to the results of Drumm & Bart [6] to 0.005 and $1.0 \cdot 10^{11}$ to fulfill the coalescence and breakage characteristics of the used system. The simulation is performed for 20 000 time steps using a time step size of 0.05 s, where the standard relaxation factors of the commercial CFD code FLUENT are used. A converged and steady state solution is reached at the end of the simulation.

4 Visualization and Results of the Eulerian Simulation

A novel approach in visualizing the Eulerian multiphase fluid simulation dataset is presented with the aim of demonstrating the dynamics of droplet movement. The simulated droplet distribution is visualized in Fig. 3a [25] based on a stochastic modeling combining the information of phase fraction and droplet size. The simulated droplet size is homogeneous for the whole compartment. Slightly smaller droplets can be seen due to numerical diffusion. Compared to literature data [26], the droplet size is slightly over-predicted by the used breakage and coalescence models. A further reduction of the coalescence kernel could lead to a better prediction of the measured droplet size data. The velocity field of the continuous phase in Fig. 3b indicates the swirl structure inside the compartment, where the velocity has its highest values at the stirrer tip. For a better understanding of the flow structure, a visualization of the droplet path through the compartment is needed.

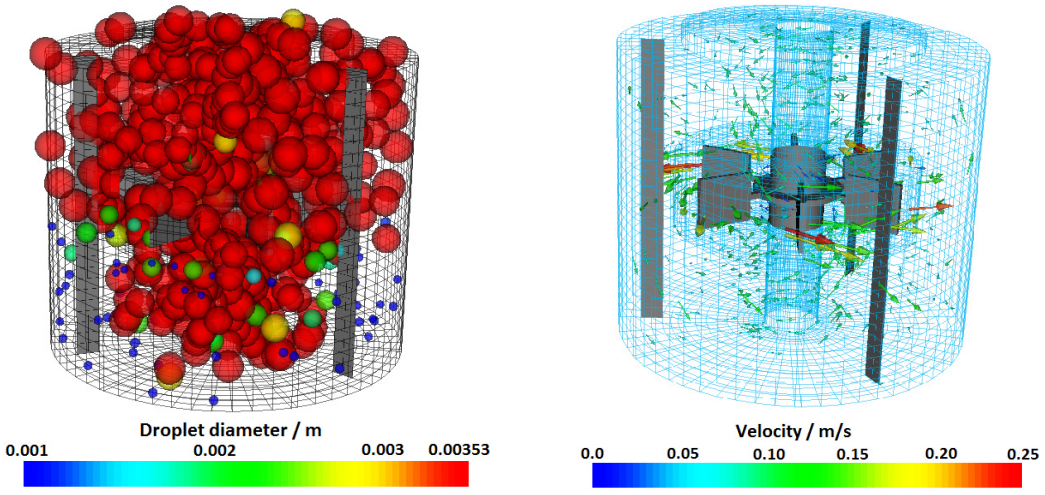

(a) Droplet distribution **(b)** Velocity field

Figure 3 Visualization of the simulation result gained by the Eulerian CFD-PBM simulation.

4.1 Path-Line Based Flow Visualization

Line integrals, such as streamlines and streak-lines are well-known representations for flow visualization [16, 17]. In the case of our particular simulation, domain experts benefit from path-lines that indicates the trace of a droplet movement over time.
A path-line denotes the trace/path of a droplet and is defined mathematically as:

$$\begin{cases} \frac{\partial}{\partial t} l(x, y, z) = \mathbf{u}(l, t), \\ l(t_0) = l_0. \end{cases} \tag{15}$$

u is the droplet velocity and l is the position of the particle. However, conventional path-line computation suffers two main deficits:

- Path-line hits mesh boundaries around stirrers and no longer continues.
- Path-line computation continues even if a droplet vanishes after a certain time point.

For simulation experts, it is important to identify flow regions with the following features:

1. regions where a droplet breaks
2. regions where droplets collide and merge.

In order to visualize these features based on a path-line representation, we propose the following coalescence and breakage detection and re-seeding method to incorporate more information into path-lines:

- Re-seeding near stirrers: if a path-line is interrupted at a mesh point near the stirrer, take another point which is near the stirrer, and start a new path-line integral from this point.
- Path-line termination after droplet interaction: Physically a trace of a droplet vanishes while the droplet itself disappears. Therefore, further integration should also be stopped after a larger droplet break. We incorporate this breakage detection into path-line integration, in order to record the life span of the droplet along its path-line.

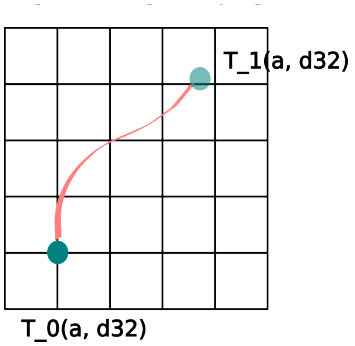

Figure 4 Path-line intergration.

We will elaborate on the path-line termination process in detail (see Algorithm 1). Suppose a droplet has position P_0 at point t_0, after time t_1, the droplet moves over to P_1, see Fig. 4. Volume fraction and particle size at each time step are given as α_i , d_i. With the help of the following detection, we test if t_1 is a time frame where a larger droplet breaks:

Algorithm 1 Adaptive path-line integration with breakup detection.

```
for each path-line do
  for t = 0 → t_i do
    if d_i/d_{i+1} > ∛2 and α_i > α_threshold then
      terminate current path-line integration,
      take a neighboring point, start a new path-line
    end if
  end for
end for
```

A droplet breakage is detected by the condition $d_i/d_{i+1} > \sqrt[3]{2}$. We assume that each droplet is a sphere with diameter d_i. Thus the volume of a droplet is given by $\frac{4}{3}\pi(\frac{d_i}{2})^3$. We further

assume a droplet will break in to two or more equal parts. Due to volume conservation, the diameter of the resulting droplet children r d_{i+1} is smaller than $\sqrt[3]{(\frac{1}{2})}d_i$. The threshold checking on volume fraction $\alpha_i > \alpha_{threshold}$ ensures that a droplet exists in this region. If a droplet breaks up, we terminate the path-line calculation at this break point. We re-seed a new point randomly within a given neighborhood. In the future, we plan to extend this re-seeding idea with further droplet breakage model, in order to provide a better location of the children droplets. Furthermore, the re-seeding of a boundary point is done by flipping the velocity vector. We assume if a particle hits the boundary, it bounces back with the same velocity magnitude and a reflecting direction.

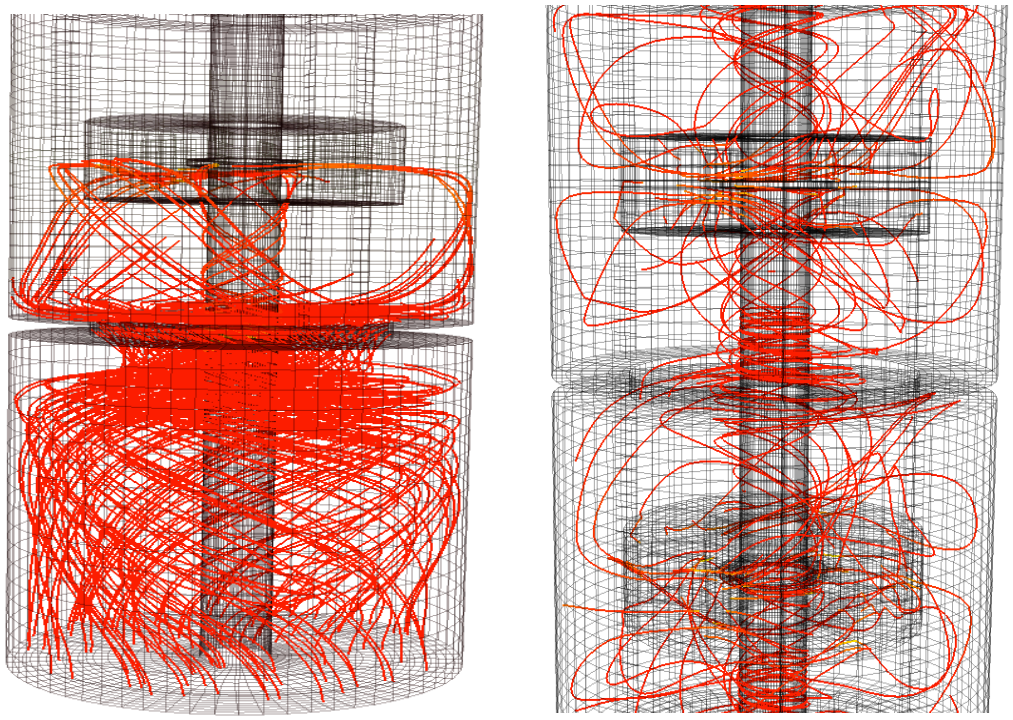

(a) Straightforward path-line integration **(b)** Path-lines with collision and bifurcation detection

Figure 5 Comparison of straight forward integration method and the particle reseeding method.

The example in Fig. 5a shows a straightforward integration without feature detection and line re-seeding. Apparently all the impaired particle paths were interrupted once they reach the stirrers. Furthermore, following all path-lines reveals the fact that no droplet breakage can be recorded. We implement our proposed re-seeding and termination criteria with a Runge-Kutta4 integration method in C++. Integration length was set smaller than the average cell size in order to obtain a smoother line output. Fig. 5b shows an example of our algorithm whose path-lines are re-seeded after droplet breakage, and integration can be continued after an interruption at the stirrer. From the presented path-line technique, the path of the droplets through the column can be visualized. Thereby, the typical double vortex structure of the flow can be seen [27].

5 Conclusions

In this paper, we presented different modeling techniques for the simulation of the hydrodynamics in extraction columns. We have shown that a full resolution of the droplet coalescence is only possible for two droplets or small number of droplets due to the required computational resources. The simulation of dispersed phase systems with thousands of droplets requires the use of simplified models. Therefore, the Eulerian model is used combined with population balance modeling to simulate the flow field as well as the changing droplet size in extraction columns. The used breakage and coalescence model for population balance modeling showed a slight over-prediction of the droplet size. Compared to the VOF method, the droplet surface is not directly tracked. Therefore, the droplets were visualized using a stochastic positioning based on the phase fraction and the droplet size. Furthermore, detection and re-seeding algorithms for droplet interactions and tracing were presented that enable the engineer to detect points of breakage and are the basis for further improvements. As future work, we will use a multi-group model that allows us the consideration of more than one droplet size in a cell. With that model, the effect of small satellite droplets that are generated during breakage can be studied. Therefore, the positioning of the droplets based on the phase fraction and droplet size will be extended to account for a stochastic visualization of the multi-group data set, which allows a direct comparison of real pictures with the visualization. In addition, a visualization of elongated droplets will help to identify these points based on the shear rate of the fluids. A visualization of the droplet movement (transient visualization) will lead to a better understanding of the start-up phase of the column. The visualization of the multi-group data will show up the position of the smaller sized droplets compared to larger sized droplets inside the compartments at one time (without using slides or probes) to reveal dead zones. Finally, the visualization of mass transfer specific data together with the droplet size data will allow combined analyses of both the interacting properties. Further investigations of different column designs (e.g. height of a compartment) will be done. Therefore, a script based mesh generation tool will be developed. The presented algorithms were only used for liquid-liquid flows, but could also be applied for the simulation and visualization of bubbly flows as it is given in bubble column reactors.

Acknowledgements The authors would like to acknowledge the financial support from DFG (Deutsche Forschungsgemeinschaft) and the State Research Centre of Mathematical and Computational Modelling (CM)^2.

A Nomenclature

c	continuous phase
d	dispersed phase
$C_1 - C_3$	model constants
C_D	drag coefficient
d_{30}	volumetric diameter
d_1, d_2	droplet diameter
f	probability density distribution function
F	surface tension force
F_r	resistance force
$g(d)$	breakup rate
g	gravity constant
h	coalescence rate
l	location of a point
m_0	zeroth moment
m_3	third moment
n	unit vector normal to the interface
N	number of droplets
p	pressure
P	probability of an eddy breaking up
P_0, P_1	position 0, position 1
S	source term
t	time
$\mathbf{u}$	velocity
V	volume
x, y, z	coordinates
α	phase fraction
ϵ	energy dissipation
κ	curvature of the interphase
λ	length of an eddy
μ	viscosity
δ	surface tension
ϕ	energy distribution function
χ	eddy viscosity/average eddy viscosity
ω	interaction frequency
τ	phase strain stress tensor

References

1 R. Andersson and B. Andersson. Modeling the breakup of fluid particles in turbulent flows. *A.I.Ch.E Journal*, 6:2031–2038, 2006.

2 C.A. Coulaloglou and L. L. Tavlarides. Description of interaction processes in agitated liquid-liquid dispersions. *Chemical Engineering Science*, 32:1289–1297, 1977.

3 R. Rieger, C. Weiss, G. Wigley, H.-J. Bart and R. Marr. Investigating the process of liquid-liquid extraction by means of computational fluid. *Computers & Chemical Engineering*, 12:1467–1475, 1996.

4 G. Modes and H.-J. Bart. CFD-Simulation der Strömungsnichtidealitäten der dispersen Phase bei der Extraktion in gerührten Extraktionskolonnen. *Chemie Ingenieur Technik*, 73, (4):332–338 2001.

5 A. Vikhansky and M. Kraft. Modelling of a RDC using a combined CFD-population balance approach. *Chemical Engineering Science*, 59:2597–2606, 2004.

6 C. Drumm and H.-J. Bart. Coupling of CFD with DPBM, drop size distributions and flow fields in a RDC extractor. *6th International Conference on Multiphase Flow*, Leipzig, Germany, July 9-13, 2007.

7 M. W. Hlawitschka, M. Mickler and H.-J. Bart. Simulation einer gerührten Miniplant-Extraktionskolonne mit Hilfe eines gekoppelten CFD-Populationsbilanzmodells. *Chemie Ingenieur Techik*, 82 (9):1389–1390, 2010.

8 C. Drumm. Coupling of Computational Fluid Dynamics and Population Balance modeling for liquid-liquid extraction. *Ph. D Dissertation*, TU Kaiserslautern, 2010.

9 C. Drumm, M. Attarakih and M. W. Hlawitschka and H.-J. Bart. One-group reduced population balance model for CFD Simulation of a pilot-plant extraction column. *Industrial & Engineering Chemistry Research*, 49 (7):3442–3451, 2010.

10 C. Martínez-Bazán, J. L. Monatenes and J. C. Lasheras. On the breakup of an air bubble injected into a fully developed turbulent flow. Part 1. Breakup frequency. *Journal of Fluid Mechanics*, 401:157–182, 1999.

11 M. J. Prince and H. W. Blanch. Bubble coalescence and break-up in air-sparged bubble columns. *A.I.Ch.E Journal*, 36 (10):1485–1499, 1990.

12 H. Luo and H. F. Svendsen. Theoretical model for drop and bubble breakup in turbulent dispersions. *A.I.Ch.E Journal*, 42 (5):1225–1233, 1996.

13 M. W. Hlawitschka and H.-J. Bart. Simulation of a miniplant kühni extraction column coupled with PBM. Proceeding ISEC 2011, 2011.

14 Goodson, M. and Kraft, M., Simulation of coalescence and breakage: an assessment of two stochastic methods suitable for simulating liquid-liquid extraction. *Chemical Engineering Science*, 59 (18):3865–3881, 2004.

15 T. Salzbrunn, C. Garth, G. Scheuermann, J. Meyer. Pathline predicates and unsteady flow structures. *The Visual Computer*, 24 (12):1039–1051, 2008.

16 C. Garth, H. Krishnan, X. Tricoche, T. Bobach and H. Joy. Generation of accurate integral surfaces in time-dependent vector fields. *Proceeding of IEEE Visualization 2008*, 14 (6), 2008.

17 A. Lez, A. Zajic, K. Matkovic, A. Pobitzer, M. Mayer, H. Hauser. Interactive exploration and analysis of path-lines in flow data. *Proceeding International Conference in Central Europe on Computer Graphics, Visualization and Computer Vision*:17-24, 2011.

18 E. Delnoij,J. A. M. Kuipers and W. P. M. Van Swaaij. Numerical simulation of bubble coalescence using a Volume of Fluid (VOF) model. *Third International Conference on Multiphase Flow*, Lyon, France, June 8th-12th, 1998.

19 D. Bothe, M. Koebe, K. Wielage, J. Pruss and H.-J. Warnecke. Direct numerical simulation of mass transfer between rising gas bubbles and water. In *Bubbly Flows:* Analysis, Modelling and Calculation (M. Sommerfeld Ed.), Heat and Mass Transfer, Springer-Verlag:159–174, 2004.

20 M. Koebe. Numerische Simulation aufsteigender Blasen mit und ohne Stoffaustausch mittels der Volume of Fluid (VOF) Methode. *Ph. D Dissertation*, Universität Paderborn, 2004.

21 F. Krause, X. Li and U. Fritsching. Simulation of droplet-formation and -interaction in emulsification processes. *Engineering Applications of Computational Fluid Mechanics*, 5 (3):406-415, 2011.

22 R. T. Eiswirth and H.-J. Bart. Untersuchung zur binären Tropfen-Tropfen-Koaleszenz in flüssig-flüssig-Systemen. *Chemie Ingenieur Technik*, 81 (8):1060, 2009.

23 C. Drumm and H.-J. Bart. Hydrodynamics in a RDC extractor, single and two-phase PIV measurements and CFD simulations. *Chemical Engineering Technology*, 29:1297–1032, 2006.

24 L. Schiller and Z. Naumann. A drag coefficient correlation. *Zeitschrift des Vereines deutscher Ingenieure*, 77:318, 1935.

25 M. W. Hlawitschka, F. Chen, H.-J. Bart and H. Hagen. CFD Simulation und verbesserte Datenauswertung einer Extraktionskolonne vom Typ Kühni. *Proc. of 1st Young Researcher Symposium (YRS) 2011*, Kaiserslautern, Germany, February 15, 2011, CEUR-WS.org, ISSN 1613-0073, online CEUR-WS.org/Vol-750/yrs04.pdf

26 T. Steinmetz. Tropfenpopulationsbilanzgestütztes Verfahren zur Skalierung einer gerührten Miniplant-Extraktionskolonne. Fortschritts-Bericht, VDI Verlag, Düsseldorf, 2007.

27 M. W. Hlawitschka and H.-J. Bart. Determination of local velocity, energy dissipation and phase fraction with LIF- and PIV- measurement in a Kühni Miniplant extraction column. *Chemical Engineering Science*, in press., doi:10.1016/j.ces.2011.10.019, 2011.